From hydrophobic to hydrophilic behaviour: A simulation study of solvation entropy and free energy of simple solutes

R. M. Lynden-Bell
Atomistic Simulation Group and Irish Centre for Colloid Science, School of Mathematics and Physics, The Queen's University, Belfast BT7 1NN, United Kingdom

J. C. Rasaiah
Department of Chemistry, University of Maine, Orono, Maine 04469

(Received 14 April 1997; accepted 30 April 1997)

We describe atomistic simulations of the free energy and entropy of hydration of ions in aqueous solution at 25 °C using a simple point charge model (SPC/E) for water and charged spherical Lennard-Jones solutes. We use a novel method with an extended Lagrangian or Hamiltonian in which the charge and the size of the ions are considered as dynamical variables. This enables us to determine thermodynamic properties as continuous functions of solute size and charge and to move smoothly from hydrophilic to hydrophobic solvation conditions. On passing between these extremes, the entropy of solvation goes through maxima. For example it shows a double maximum as a function of charge at constant size and a single maximum as a function of size at constant (non-zero) charge. These maxima correspond to extremes of structure-breaking and are associated with the disappearance of the second solvation shell in the radial distribution function; no anomalies are seen in the first shell. We also present direct evidence of the asymmetry in the free energy, enthalpy and entropy of hydration of ions on charge inversion arising from the asymmetry in the charge distribution in a water molecule. Our calculation only includes local contributions to the thermodynamic functions, but once finite size corrections are applied, the results are in reasonable agreement with experiment. © *1997 American Institute of Physics.* [S0021-9606(97)50730-6]

I. INTRODUCTION

Water is the most ubiquitous solvent on earth. It is an unusual liquid with a remarkably high dielectric constant and a low coordination number. At the molecular level many of its properties may be ascribed to the distribution of charge within the molecule which results in it being able to form four hydrogen bonds, two donated and two accepted. The fact that the molecule is polar favours the solvation of charged and polar species while the fact that the charge distribution is more complex with higher multipole moments tends to favor the formation of a hydrogen-bonded network which is the source of many of the unique properties of ice and liquid water.[1–6]

This paper is part of a detailed study of the thermodynamics, structure and mobility of simple solutes in a model of water using atomistic simulation. Our aim is to use the freedom available in simulations to vary parameters independently to make a thorough study of the effects of solute size and charge on these properties. We hope to gain insight into the relationship between hydrophilic and hydrophobic solvation,[4,6] the differences of mobility of positively and negatively charged ions and to attempt to explain at a molecular level why small ions move more slowly than faster ones.[7–9] This paper will concentrate on the thermodynamics of solvation. In particular we describe a new application of the extended Lagrangian technique which gives the variation of free energy and entropy of solvation as functions of solvent size and charge, allowing us to move from hydrophilic to hydrophobic solvation in a continuous way. This enables us to follow the asymmetry in the free energy and entropy of hydration of ions on charge inversion which arises from the asymmetry in the charge distribution in a water molecule.[10]

The use of simulation to study solvation in aqueous solutions is well established. For example Impey *et al.*[11] studied the structure and dynamics of ions in water in 1983 while Pangali *et al.*[12] studied methane in water in 1979. The importance of the role of entropy in hydrophobic solvation has been re-emphasized recently by Haymet,[13,14] while the use of the concepts of structure-breaking and structure-making to explain the varying entropies of solvation of ions was proposed by Frank[15,16] and is discussed in some detail by Gurney.[17] The elucidation of free energy differences due to changes in intermolecular interactions is an important problem in solution chemistry which can be studied by computer simulation using a number of methods[18] such as the slow growth method and thermodynamic perturbation theory. In these methods one follows the alchemic transformation or slow growth of molecules in a computer simulation to provide the free energy differences directly. The total free energy change in the transformation from state A to B is obtained as the sum over smaller changes between adjacent states. This requires a large number of separate equilibrium simulations corresponding to several intermediate states and many technical modifications to improve the accuracy and efficiency are described in the literature.[18–21] The calculations are simple though tedious and have provided the free energies of ligand binding,[22–24] and solvation of ions,[25–28] non-polar solutes[29–35] and amino acids.[36]

The novel aspect of the work described in this paper is that we have measured the entropy, free energy and energy

of solvation as a continuous function of solute charge and size, enabling us to span the hydrophobic and hydrophilic solvation regimes. The method we use has an extended system dynamics in which the free energy changes are calculated on the fly and which allows us to determine entropy changes as well. It is a more efficient procedure for our purposes, which are to study free energy and entropy differences accompanying variations in the charges and sizes of ions and their correlation with their transport properties. We calculate the effects due to the molecular nature of the solvent which are local to the ion (say in the first two solvation shells). Some sort of finite size correction must then be applied to account for the effects of longer range interactions, but these can be described by a simpler model. The most interesting results relate to the variation of entropy of solvation where the long range effects are small.

II. MEASURING THE FREE ENERGY OF SOLVATION

A. Free energy measurements

In order to understand exactly what we measure in the simulation let us first consider the Born model[17,37–39] for solvation of a charged sphere radius r in a uniform medium with dielectric constant ϵ. The work done in charging the sphere in vacuum is the free energy A_{vac} of an isolated charged sphere and is given by

$$A_{vac}=\frac{q^2e^2}{8\pi\epsilon_0 r}, \tag{2.1}$$

where q is the charge of the ion in units of the proton charge e, ϵ_0 is the permittivity of free space and r is the radius of the ion. As there is no change of entropy associated with this process, this is equal to the energy, U_{vac}, which is conventionally described as being stored in the field. The work done in charging a sphere of the same size in a medium is reduced by the inverse of the dielectric constant, which gives the free energy of a charged sphere in a medium as

$$A_{med}=\frac{q^2e^2}{8\pi\epsilon_0\epsilon r}. \tag{2.2}$$

The solvation free energy is associated with the polarisation of the dielectric and is the difference of these quantities,

$$A_{solv}=A_{med}-A_{vac}=-\frac{q^2e^2}{8\pi\epsilon_0 r}(1-\epsilon^{-1}). \tag{2.3}$$

Thus in the Born model the solvation free energy is negative and increases quadratically with the charge and decreases as the inverse of the radius. It can be divided into energetic and entropic terms by taking the derivative with respect to temperature, giving

$$S_{solv}=-\frac{q^2e^2}{8\pi\epsilon_0 r}\left(\epsilon^{-2}\frac{d\epsilon}{dT}\right), \tag{2.4}$$

$$U_{solv}=-\frac{q^2e^2}{8\pi\epsilon_0 r}\left(1-\epsilon^{-1}+T\epsilon^{-2}\frac{d\epsilon}{dT}\right). \tag{2.5}$$

Experimentally for water at 298 K[40] $\epsilon=78.358$ and $d\ln\epsilon/dT=-1.3679\ \mathrm{K}^{-1}$ giving $A_{solv}=-686q^2/r\,\mathrm{kJ\ mol}^{-1}$ and $S_{solv}/k=-4.9q^2/r$, where q is the charge in units of the proton charge and r is the radius in Å. In this model both the entropy and the energy vary as q^2/r, and positive and negative ions behave in the same way.

In practice, we perform simulations using periodic boundary conditions with periodically repeated images, so that we must consider the additional process of forming the lattice from the charged ions. In the vacuum the work done to form such a Wigner lattice[41,27] is given by

$$A_{lat}=-\frac{\zeta q^2e^2}{8\pi\epsilon_0 L}, \tag{2.6}$$

where ζ is a constant whose value depends on the lattice and L is the separation between an ion and its nearest image. For a simple cubic lattice $\zeta=-2.837\,297$,[41] while for an fcc lattice such as we use in this work $\zeta=-3.2420$.[42] When the same process is performed in a medium with dielectric constant, the work done is reduced by a factor of ϵ. Thus the measured solvation energy in a periodic lattice with a dielectric medium is

$$A_{solv,lat}=-\frac{q^2e^2}{8\pi\epsilon_0}(1-\epsilon^{-1})(r^{-1}-\zeta/L). \tag{2.7}$$

As the lattice size is increased the term in ζ/L goes to zero and the desired result for infinite dilution recovered. We shall use this expression to correct our results for finite size effects assuming that our system is large enough that the long range corrections can be described by a uniform dielectric constant. Hummer *et al.*[27] have shown that applying this kind of correction brings results from many different system sizes into good agreement, even for cubic systems with only 32 or 64 molecules. It seems that they did not include the small term in the inverse of the dielectric constant which is negligible in aqueous systems.

We used the technique to be described in the next section to measure the variation of the Helmholtz free energy, A, with solute charge and size of an ion in a molecular model of water. The question is whether we are measuring the solvation energy, A_{solv} or the free energy associated with charging a sphere in a medium, A_{med}. Although we do charge the solutes in the medium, we do not include any self energy in the Hamiltonian so that if the method were to be applied in the absence of a solvent no change in free energy would be recorded. Thus we are measuring changes of $A_{solv,lat}$, the free energy associated with the interaction of the solute with the medium. The corresponding internal energy can be measured directly as a function of charge and size. It is made of two parts, the direct solute–water interaction energy, U_{SW}, and changes in the water–water interaction energy, U_{WW}. These were measured separately. However the combination of periodic boundary conditions and the Ewald summation means that the water molecules ''feel'' the ion and all its images; we need to choose the box to be large enough that the water molecules in the first two solvation shells interact considerably more strongly with the nearest ion than with its

images and then apply a correction for the longer range effects. If too large a system is chosen computation becomes less efficient and the determination of changes in the potential energy of the water–water interactions less accurate. If too small a box is chosen the phenomena which are associated with the molecular structure of the solvent will be perturbed.

B. An extended Lagrangian method for measuring relative free energies and entropies as a function of ion charge and size

In order to measure the changes of A_{solv} with charge and solute size we use a mathematical trick to relate the free energy of a system with a specified charge and size to probabilities in an artificial system in which the charge and size are treated as dynamical variables. The use of extended systems with artificial dynamical variables with fictitious masses is well established in molecular dynamics.[43,44,18] Examples include the Nosé thermostat[45] and the Car-Parrinello *ab initio* method.[46] This application differs from previous ones in the information we seek to extract from the extended system. We do not look for averages of quantities such as the energy or the pair correlation function in the extended system — indeed these have no physical meaning in the real world. What we do is to consider the charge and solute size as order parameters in the extended system and construct the Landau free energy in this system as a function of these variables. We can show that the Landau free energy in the extended system is identical to the Helmholtz free energy of real systems in which the charge and solute size are fixed.

The Hamiltonian in the extended system is equal to the Hamiltonian for the real system augmented by kinetic energy terms for the solute charge q and size σ

$$H=V(q,\sigma,\{\mathbf{r}_i\})+T+\frac{1}{2m_q}p_q^2+\frac{1}{2m_\sigma}p_\sigma^2, \tag{2.8}$$

where p_q and p_σ are momenta associated with the new variables q and σ and m_q and m_σ are the associated fictitious masses. V and T are the potential and kinetic energies respectively. The equations of motion that one derives from this Hamiltonian are the standard equations of motion for the positions and velocities augmented by

$$\dot{q}=p_q/m_q,\quad \dot{\sigma}=p_\sigma/m_\sigma,\quad \dot{p}_q=F_q=-\frac{\partial V}{\partial q},$$
$$\dot{p}_\sigma=F_\sigma=-\frac{\partial V}{\partial \sigma}. \tag{2.9}$$

The fictitious forces acting on the charge and size variables depend on the form of the potential energy of interaction between the solute and the water. It is often convenient to add a biasing potential $V_{bias}(q)$ or $V_{bias}(\sigma)$ to the Hamiltonian which gives additional terms in the forces on the extended variables.

In the canonical ensemble of the extended system the probability of finding the configuration variables $\mathbf{r}\equiv\{\mathbf{r}_i\}$ with values between $\mathbf{r}_0$ and $\mathbf{r}_0+d\mathbf{r}$ and the new variables with values between q_0,σ_0 and $q_0+dq,\sigma_0+d\sigma$ is given by

$$p(\mathbf{r}_0,q_0,\sigma_0)d\mathbf{r}dqd\sigma$$
$$=Z^{-1}\exp[-V(\mathbf{r}_0,q_0,\sigma_0)/kT]d\mathbf{r}dqd\sigma, \tag{2.10}$$

where we have integrated over all the momenta (real and fictitious) and defined the configurational integral Z in the extended system by

$$Z=\int\int\int \exp[-V(\mathbf{r}_0,q_0,\sigma_0)/kT]d\mathbf{r}dqd\sigma. \tag{2.11}$$

If we now integrate over the positions (note that in our notation $\mathbf{r}$ denotes the 3N-dimensional vector of all positions) we obtain an expression for the probability of finding the system with a specific charge and size

$$p(q_0,\sigma_0)dqd\sigma$$
$$=Z^{-1}\left\{\int \exp[-V(\mathbf{r}_0,q_0,\sigma_0)/kT]d\mathbf{r}\right\}dqd\sigma. \tag{2.12}$$

However, if we had a canonical ensemble of real systems with $q=q_0,\sigma=\sigma_0$ the statistical mechanical expression for the Helmholtz free energy would be

$$\exp[-A/kT]=\int \exp[-V(\mathbf{r}_0,q_0,\sigma_0)/kT]d\mathbf{r}, \tag{2.13}$$

which is just the integral in the curly brackets in the preceding equation for the probability of finding the values q_0,σ_0 in the extended system. Thus in the extended system

$$p(q_0,\sigma_0)dqd\sigma=Z^{-1}\exp[-A(q_0,\sigma_0)/kT]dqd\sigma \tag{2.14}$$

or

$$A(q_0,\sigma_0)=-kT\ln p(q_0,\sigma_0)+constant. \tag{2.15}$$

This shows that the Landau free energy $A(q_0,\sigma_0)$ in the extended system is equal to the actual free energy of a real system with the corresponding values of the variables, and gives us a way to calculate it.

In order to construct the free energy surface $A(q,\sigma)$ we need to have a series of configurations which are representative of a canonical ensemble of the extended system. This could be done with a Monte Carlo simulation, but we used molecular dynamics. In a molecular dynamics simulation the momentum variables exchange energy with the configurational variables, so that if one applies a thermostat to the momenta the configurations generated by the equations of motion should be representative of a canonical ensemble. The relative probabilities of different charges and sizes are then found by constructing histograms. Experience in similar work[20,18] has shown that the noise can be reduced by using a biasing potential, U_{bias}, which depends only on the order parameters (in this case q and σ) and which restricts the range of values of the order parameters sampled in any one run. Samples from different windows are joined to construct the overall Landau free energy function. It can easily be shown that if there is a biasing potential, U_{bias}, present

TABLE I. Potential parameters used for ion–water interaction.

Ion	ϵ/kJ mol^{-1}	σ_{SO}/Å
Na^+	0.5216	2.876
K^+	0.5216	3.250
Cs^+	0.5216	3.526
Cl^-	0.5216	3.785
Br^-	0.4948	3.896
I^-	0.5216	4.168

$$A(q_0,\sigma_0) = -kT\ln p_{bias}(q_0,\sigma_0) - U_{bias} + constant. \tag{2.16}$$

III. TECHNICAL DETAILS

A. Potentials

The water potential used was the revised SPC/E model of Berendsen *et al.*[47] which has partial charges on the protons and the oxygen nucleus and a Lennard-Jones site on the latter. The molecule is rigid. The solutes are modelled as charged or uncharged Lennard-Jones spheres, and, as there is only one solute molecule in the simulation cell, only the potential for the interaction of the solute with water is needed. This is described by three parameters, the charge and the values of the Lennard-Jones parameters ϵ_{SO}, σ_{SO}. We chose a constant value for ϵ_{SO}, namely $\epsilon_{SO}=0.5216$ kJ mol^{-1} which is equal to the value given by Dang[48] for the ions Na^+, K^+, Cs^+, Cl^-, Br^- and I^-, and used in our previous work.[7,49] Table I gives values for the σ_{SO} parameters for these ions and for the water potential. Using the Lorentz–Berthelot combining rules the value of σ_{SO} can be related to the diameter of the solute σ_{SS} by

$$\sigma_{SS} = 2\sigma_{SO} - 3.169 \ \text{Å}. \tag{3.1}$$

In the simulations σ_{SO} was used as the variable describing the solute size, but the results are presented in this paper as a function of the solute diameter, σ_{SS}.

With this potential the forces acting on the fictitious variables are given by

$$F_q = -\frac{\partial V}{\partial q} = -\sum_i \frac{q_O}{4\pi\epsilon_0 r_{si}} - \sum_j \frac{q_H}{4\pi\epsilon_0 r_{sj}} = -U^{coul}_{solv}/q, \tag{3.2}$$

$$F_\sigma = -\frac{\partial V}{\partial \sigma} = -\sum_i \frac{4\epsilon_{SO}}{\sigma_{SO}}\left[12\left(\frac{\sigma_{SO}}{r_{Si}}\right)^{12} - 6\left(\frac{\sigma_{SO}}{r_{Si}}\right)^{6}\right]. \tag{3.3}$$

In these expressions the sums over i are over all oxygen sites and those over j are over proton sites. The fictitious force on the charge is just minus the ratio of the coulomb part of the solvation energy to the instantaneous charge (which is the electrostatic potential at the ion due to the solvent), and can conveniently be calculated with the electrostatic energies and forces, while the fictitious force on the size is related to part of the Lennard-Jones contribution to the virial and is calculated at the same time as the Lennard-Jones forces and energies.

B. Simulation conditions

The program was adapted from DLPOLY.[50] In part of the work the equations of motion were integrated with a time step of 1 fs using quaternions to describe the orientations of the water molecules. We then realised that, as equilibrium properties are independent of mass, one may replace the protons by particles of mass 8 amu (or any other mass); this allowed us to increase the time step to 2.5 fs. The solute mass was set equal to 23 amu for all runs. The system size was chosen to be large enough to contain the first two solvation shells around the solute, with half the separation between a solute and its nearest image equal to 6.9514 Å. The repeated unit was arranged in an fcc lattice, giving a truncated dodecahedral simulation cell. These periodic boundaries give the maximum separation of images for a given volume, and our cell contains only 64 molecules, which allowed us to perform many long runs to get good statistics for energies and populations.

Long range electrostatics were evaluated with an Ewald sum with a convergence parameter of 0.53 Å^{-1} and 8 k vectors in each direction. A cutoff of 6 Å was used for evaluation of the Lennard-Jones and real space electrostatic terms. As the system contains a net charge, the true electrostatic energy would be infinite due to the repulsion between charges and their images. There is, however, no force on the charge due to its own images so the way in which these terms are treated makes no difference to the structure or dynamics of the confidurational variables. In this work we omitted all interactions between the charge of the solute particle and its images. The effect on the equations of motion of the charge is equivalent to adding a quadratic biasing potential. However, as we are interested in the free energy stored in the medium surrounding a single ion, such terms should properly be omitted, although they must be considered before making contact with experiment.[27]

Although we have described the method in general terms with both charge and size varying, it is more convenient in practice to allow one or other of these variables to vary, taking constant q and constant σ cuts across the surface $A(q,\sigma)$. The values used for these investigations were $q=-1$, 0 and 1 for the cuts at constant q and σ_{SO}/Å $=2.876$, 3.526, 4.168 which correspond to the sizes of Na^+, Cs^+ and I^- for the cuts at constant size. The positions of these cuts in (σ,q) parameter space are shown in Fig. 1. In most of the simulations the values for the fictitious masses were chosen to be $m_q=2000$ kJ mol^{-1} ps electron^{-2} and $m_\sigma=5\times10^4$ kJ mol^{-1} ps Å^{-2}.

In the runs in which charge was varied, windows of $0.4e$ were used with run lengths of at least 250 000 steps and more generally 400 000 steps. In the runs where size was varied, windows of 0.5 Å were used and runs were of similar length. Each window was divided into 100 bins for the construction of histograms. The runs at constant size and charge used for finding radial distribution functions were 100 000 steps or longer.

For each window of values of the charge or size a histogram was constructed of the number of times the values of

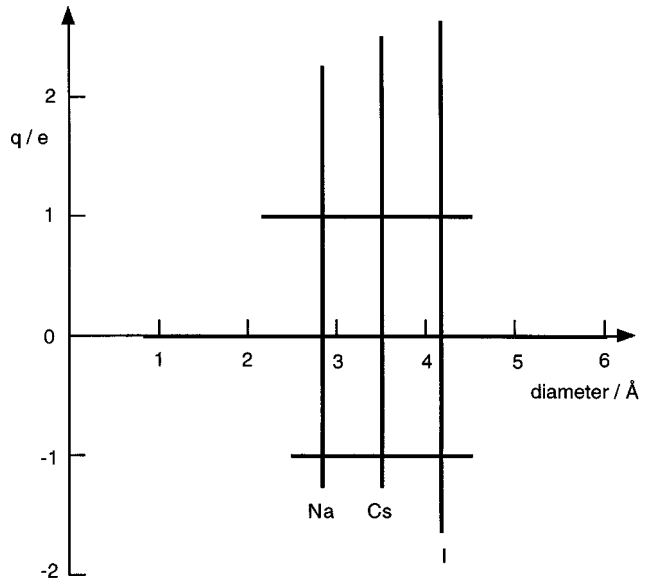

FIG. 1. Diagram showing the (q,σ) parameter space. The three vertical and three horizontal lines show the paths followed in the six numerical experiments.

the relevant parameter was in a certain range. At the same time values of the solvent–water potential energy, the water–water potential energy, the system kinetic energy, and the force F_q or F_σ on the order parameter were accumulated for each bin of values of the charge (or size). At the end of the run these were converted into averages to give $U(q,\sigma)$, etc. The free energy within the window was found from Eq. (2.14). Finally the complete free energy curve was constructed by joining the results from runs with different windows.[20,18] There are several checks on this process. First it is essential that the canonical phase space is properly sampled, i.e. that the system has equilibrated. A good check on this is that the kinetic energy does not vary with q and that the average kinetic energy of the charge or size variable is equal to $kT/2$. A further check on the equilibration and the construction of the free energy curve is to compare the free energy obtained by integrating the force $F_q(q)$ with the one obtained from the histograms. These were found to agree well. A final test for consistency is to combine the results from constant q and constant size runs, where four parameters must be chosen to fix the nine crossing points of the constant size and constant charge cuts as consistently as possible. The discrepancies were of the order of ± 3 kJ mol^{-1} or better.

These methods give relative values of the free energy and entropy. These were converted to absolute values in three stages. First the size-variation of A for uncharged solutes was extended to a smaller and unphysical value $\sigma_{SO}=1$ Å. Then the value of the Lennard-Jones parameter ϵ_{SO} was reduced in steps to $\epsilon_{SO}=0.1$ kJ mol^{-1} and the changes in A determined by thermodynamic perturbation theory. Finally the main program was run with this value of ϵ_{SO} for σ varying between 1 Å and 0.1 Å. The upper bound of the entropy for a 0.1 Å solute can be calculated assuming the free volume to be $V-4\pi N\sigma^3/3$. This is negligible. The

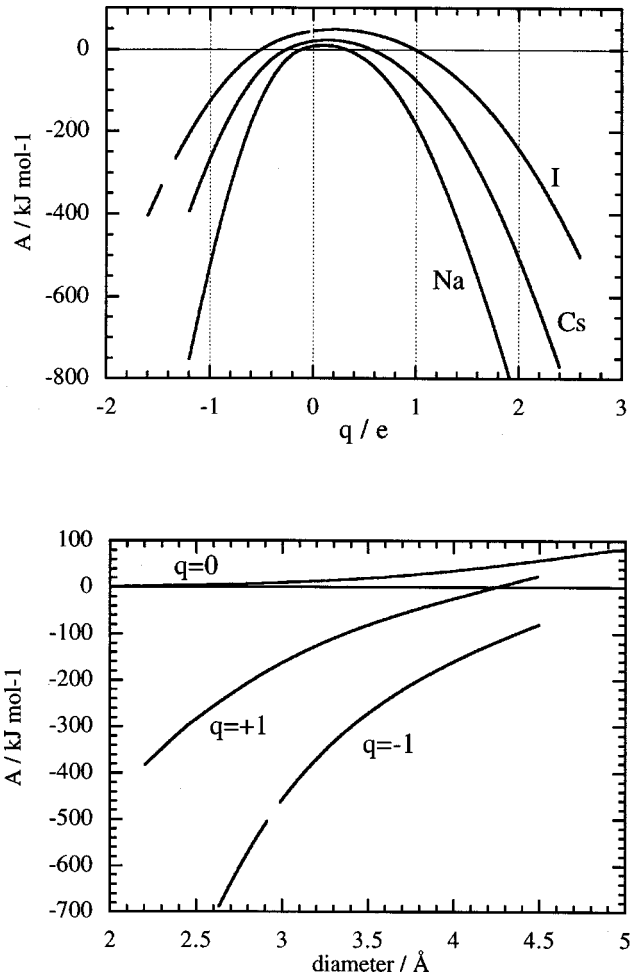

FIG. 2. The variation of solvation free energy $A(q,\sigma)$ with charge (above) and size (below). In the upper part of the diagram the curves belong to the sodium, caesium and iodine families with diameters 2.876, 3.25, and 4.126 Å respectively. In the lower part of the figure the curves belong to $q=0,+1$ and -1.

total correction gave $A_{solv}(\epsilon_{SO}=0.5216,\sigma=1,q=0) = -0.25$ kJ mol^{-1}. Within the errors of determining the energy, this is purely entropic and the total correction is less than the uncertainly in A and S.

Once $A(q,\sigma)$ is known, $S(q,\sigma)$ can be calculated from

$$S(q,\sigma)/k=[U(q,\sigma)-A(q,\sigma)]/kT. \tag{3.4}$$

The entropy curves are quite noisy and checks for consistency in this quantity were less satisfactory. The main source of noise was found to be in the water–water potential energy where one is measuring small changes in a comparitively large quantity. A considerable reduction of the noise, especially for small charges, was obtained by fitting the water–water potential energy with a polynomial function and using this in the construction of the entropy curves.

IV. RESULTS

A. Free energy and entropy

Figure 2 shows the variation of the local free energy of solvation $A(q,\sigma)$ with charge (above) and with size (below).

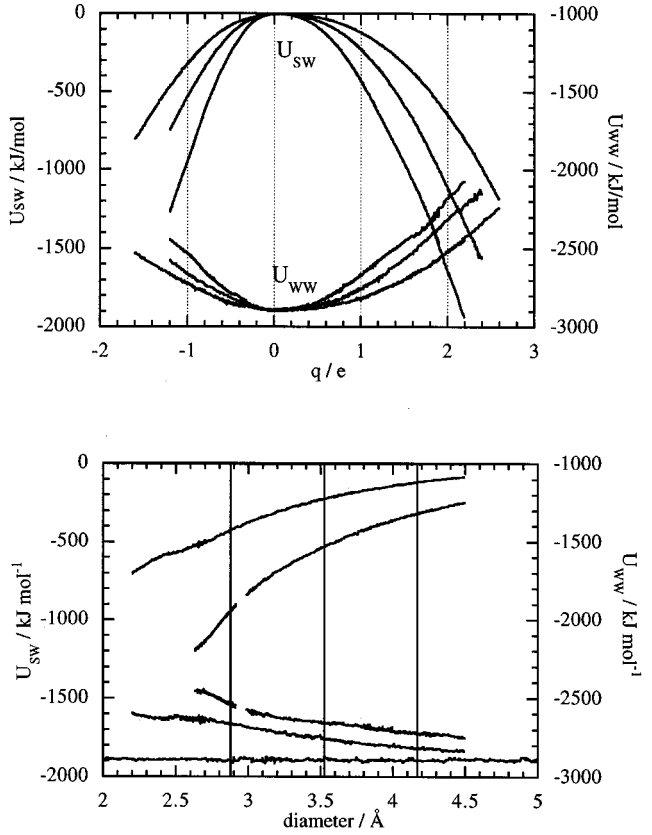

FIG. 3. The variation of solvation energy $U(q,\sigma)$ with charge (above) and size (below). In each part of the figure the upper set of three curves show the potential energy of the direct solute–water interaction and refer to the left hand ordinate, while the lower sets of curves show the total water–water interaction energy and refer to the right hand ordinate. The energy scales are the same, but the origins are shifted relative to each other. In the upper figure the steepest curves belong to the sodium family, the middle ones to the caesium family and the outer ones to the iodine family. In the lower part of the figure the curves belong to $q=0$ (flattest), $+1$ and -1 (steepest) respectively.

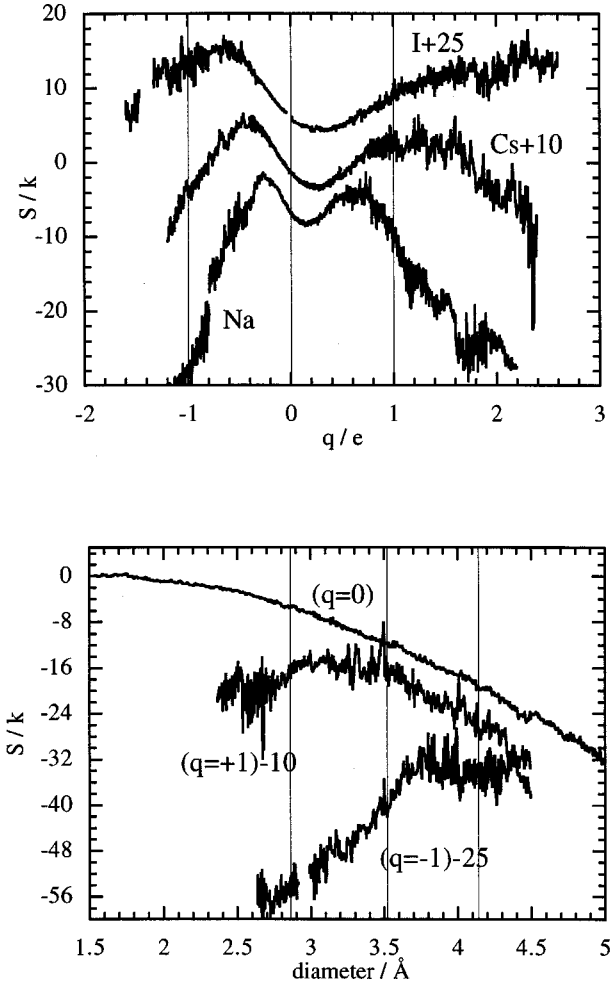

FIG. 4. Variation of solvation entropy with charge (above) and size (below). Note that the curves are displaced by the amounts shown for clarity.

In each graph the relative positions of the curves are fixed from the other set of runs as described above. As described in Section II A in a continuum model this should be proportional to the square of the charge and proportional to the inverse of the solute diameter minus a constant [see Eq. 2.7]. While this describes the overall trends approximately, there are important discrepancies which we can attribute to the fact that the solvent is molecular in nature. Firstly there is a marked difference between positive and negative charged solutes of the same size. This can be seen most clearly in the lower figure where, for a given size, it can be seen that negative ions have almost twice the solvation free energy as positive ions of the same size. The maximum in the free energy curves as a function of charge lies at small positive values of q rather than at $q=0$. These observations show that the molecular structure of the solvent is important, and that water does not behave as a simple dipolar solvent. There is also a small change of free energy with size for uncharged (hydrophobic) solutes, which we find is mainly entropic.

Figure 3 shows the two contributions to the potential energy, the direct solute–water energy U_{SW} and the total water–water interaction energy U_{WW}. We see that the variations in these two quantities oppose each other; as the charge increases from zero the direct interaction becomes more negative but the water–water energy increases. In the figures the energy scales for these two quantities are shifted, but cover the same range, so that it is apparent that the change in the direct solute–water interaction is about twice as great as the change in the water–water interaction. The net effect is a stabilisation of solvation as the magnitude of the charge increases. Once again there is an asymmetry between positive and negative charges. The variation of potential energy with solute size for uncharged solutes is too small to see on the scale of these figures.

The entropy was determined from the curves for A and U by subtraction and then by setting the entropy of an uncharged solute with size $\sigma=0.1$ Å equal to zero (see discussion in the previous section). The results are shown in Fig. 4 in units of Boltzmann's constant k. These curves seem much noisier than the ones for the energies and free energies. This is in part because the main contribution to the free energy is from the energy, and variations in $-ST$ are comparitively small. Fluctuations of ± 4 in the entropy expressed in units

of Boltzmann's constant correspond to fluctuations of ± 10 kJ mol^{-1} in the difference $(A-U)$ of the energies shown in Figs. 2 and 3, and the whole range of entropy variation in Fig. 4 corresponds to about 50 kJ mol^{-1} in ST.

Considering first the variation with charge (upper curves), we see in every case a double maximum structure with a central minimum for small positive charges. These curves show in one sweep the whole range of behaviour from hydrophobicity to hydrophilicity. The minimum corresponds to a comparitively ordered arrangement of the water structure around a neutral solute or slightly positively charged solute which we shall refer to as hydrophobic ordering. As the magnitude of the charge is gradually increased, the hydrophobic order is disrupted and the entropy increases (although in every case the entropy of solvation is still negative). This effect is known as structure-breaking and the result of disruption of the hydrogen-bonded network which also causes the increase in the water–water potential energy seen in Fig. 3. As the charge is increased still further the molecules in the solvation shells become ordered due to the field of the solute, and eventually this decrease of entropy is greater than the increase in entropy that due to structure-breaking (note that the water–water potential energy continues to increase) and the total entropy decreases. This we shall term hydrophilic ordering.

In the lower part of Fig. 4 we see that the hydrophobic order around uncharged solutes increases with solute size. The size dependence for ions with charge of both $+1$ and -1 increases for small sizes, reaches a maximum and then decreases. There is a difference between positive and negative ions, with the latter reaching a maximum at larger sizes. These maxima correspond to the crossover from hydrophilic order (in the small ions) to hydrophobic order (in the large ions).

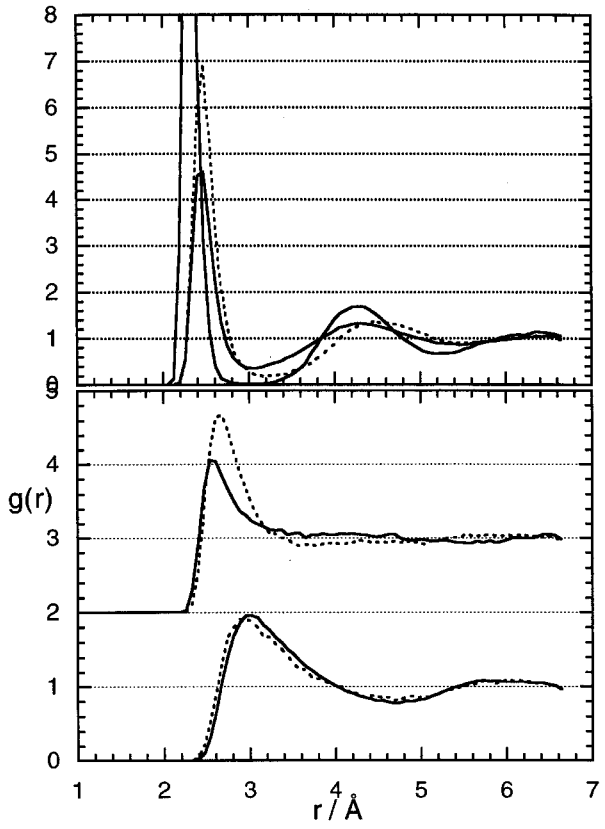

FIG. 5. Plot of radial distribution functions for the solute–oxygen distribution for the sodium family. The upper set of three curves are for examples with low entropy due to hydrophilic order ($q=-1,+1$ and -0.5 - dashed line); the middle set belong to values of the charge near the entropy maxima ($q=-0.3$ - dashed, $+0.5$) and the lower curves correspond to regions of low entropy due to hydrophobic order ($q=0$, $q=+0.2$ - dashed).

B. Structure

In order to understand the variation in thermodynamic functions, and in particular the variation in entropy as a function of solute charge, we examined radial distribution functions as a function of distance from the solute for a number of solutes in the sodium family, that is atoms with the same size as Na^+ but with different fixed charges. Figure 5 shows the radial distribution functions $g_{SO}(r)$ for the solute–oxygen internuclear distance. The values for q are $q=\pm 1$ and $q=-0.5$ (top graphs), $q=+0.5$ and -0.3 (middle graphs) and $q=0,+0.2$ (bottom graphs). The examples in the bottom graphs are near to $(q=+0)$ or at $(q=+0.2)$ the minimum entropy of solvation and the examples in middle graphs are both close to maxima in the solvation entropy.

Focusing our attention on the first peak in the radial distribution function, we see that as $|q|$ increases this peak sharpens and moves towards the solute. We do not see any anomalous behaviour in this peak as the entropy goes through a maximum value. The coordination number does not vary monotonically. The first shell contains 6 water molecules for ''Na^{-1}'' and just under 6 molecules for Na^{+1}. The shell for ''$Na^{-0.5}$'' is well defined and contains approximately four water molecules; the remaining species have less well defined first shells with higher coordination numbers.

It is the second shell which shows differences between high and low solvation entropy. The two examples with maximum solvation entropies ($q=+0.5$ and $q=-0.3$) in the central graphs have no visible second shell in $g(r)$. The hydrophobic solutes ($q=0.0$ and $q=+0.2$) have a quite well developed second shell at about 6.2 Å, which disappears as the magnitude of the charge is increased and eventually is replaced by a second shell around 4.3 Å in the top graphs. Thus the structure-breaking effect which is evident in the solvation entropy seems to be associated with the second solvation shell rather than the first shell. Further evidence for this statement is shown by a similar lack of a second solvation shell in the radial distribution function for $Cs^{-0.5}$, another species near a maximum in the solvation entropy curves (the graphs are not shown here, but our observations confirm those for $Cs^{-0.5}$ in Ref. 27).

Figure 6 shows the electrostatic potential of the solvent at the ion. This does not include the term proportional to q which arises from finite size corrections, which would increase the slope of these curves. As Hummer *et al.*[27] observed the electrostatic potential is positive for uncharged solutes due to the asymmetry of the water molecule. The

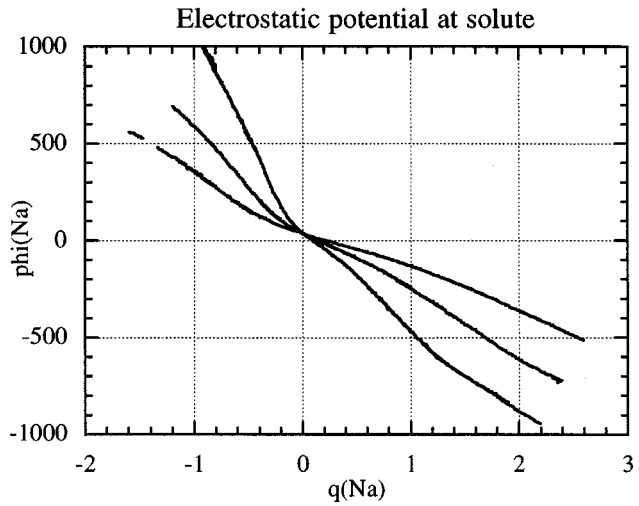

FIG. 6. Variation of electostatic potential at the ion with charge. The steepest curve belongs to the sodium family, the middle curve to the caesium family and the shallowest curve to the iodide family.

curves are not linear, although linear regions can be seen.

More information about the polarisation of the shells is contained in Fig. 7 which shows the differences between the radial distribution functions for solute-protons and solute-oxygen weighted with the factor 0.8476. As the oxygen nucleus carries a charge of 0.8476 and the protons half this charge, this weighted difference is proportional to the local charge density in the solvent, and gives some measure of the orientational order in the solvation shells. Molecules in the first shell of a solute with charge of $+1$ are oriented in the expected way with the oxygen atoms nearer the positive ion and protons between the oxygen atoms of the first and second shell. In the shells near the negatively charged ion one finds, as expected, a positive peak of protons inside the negative peak associated with oxygen atoms, but between the shells there is a double peaked positive contribution which arises from the second proton in the outer shell at about 2.4 Å and a peak at about 4.3 Å arising from protons attached to water molecules in the second shell. Looking next at the uncharged solute one sees that there is still a slight preference for protons to be nearer the solute that oxygen atoms (note the change of scale). As the charge becomes more positive this orientational preference is reversed and by the time the charge reaches $+0.5e$ the first peak with a positive charge density has almost disappeared. These plots do not show any special features that can be correlated with the entropy maxima.

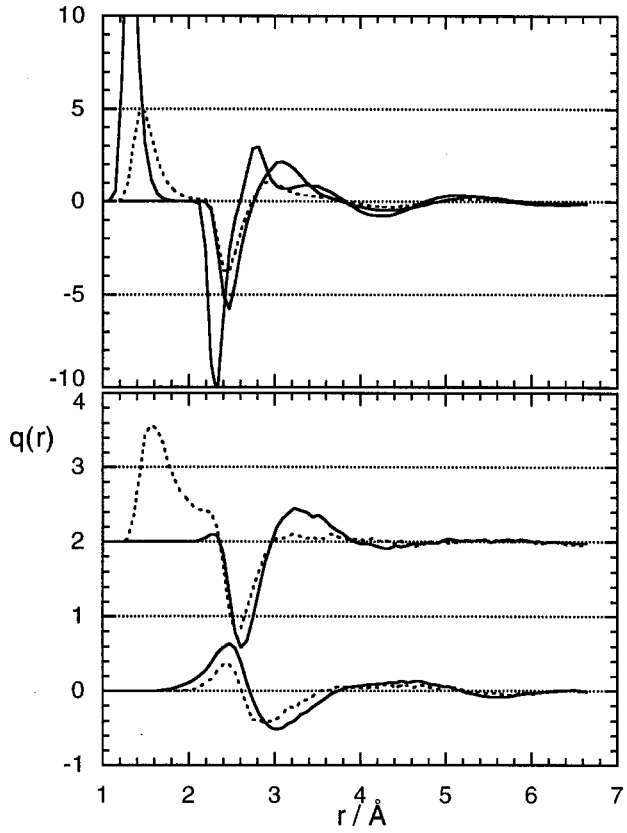

FIG. 7. Plots of the difference of the solute–hydrogen and solute–oxygen distribution functions. In this model this corresponds to the charge density. The upper set of three curves are for examples with low entropy due to hydrophilic order ($q=-1,+1$ and -0.5 - dashed line); the middle set belong to values of the charge near the entropy maxima ($q=-0.3$ - dashed line ,$+0.5$) and the lower curves correspond to regions of low entropy due to hydrophobic order ($q=0$, $q=+0.2$ - dashed line).

V. DISCUSSION

A. Hydrophilic and hydrophobic solvation: Concepts and behaviour

As the charge is varied in this model, the solute changes from a spherical hydrophobic solute to a typical hydrophilic ion. Simple uncharged Lennard-Jones spheres have been used extensively to model the solvation of both argon and methane in water, while Lennard-Jones spheres with charges of plus or minus 1 or 2 have been used in simulations of ions in water. Thus our system has the complete range of behaviour from hydrophobic solvation to hydrophilic solvation. When a hydrophobic solute dissolves in water there is normally a considerable decrease in entropy and a small decrease in enthalpy. The reason for the low solubility of such solutes is primarily the negative entropy of solvation which has been associated with the ordering of the water structure around the solute. An extreme example of this order is found in clathrate compounds of solutes such as methane in water. We found a steady decrease in the entropy of solvation and correspondingly an increase in the free energy of solvation as the size of the solute increased, which is consistent with the formation of an ordered layer of water around the surface of the solute. As the volume of such a shell increases as the square of the radius of the solute one might anticipate that the hydrophobic solvation entropy might decrease as the square of the radius of the shell, although this is partially offset by the effect of the curvature of a hydrophobic surface on free energy of hydrophobic solvation.[33,34] Our calculations suggest that it is not only the first shell that is important, but the second shell is also a significant factor. The evidence for this statement arises from the changes seen in $g(r)$ when the solute charge is turned on and the solvent

becomes more hydrophilic. The entropy maxima are associated with the disappearance of a distinct second solvation shell, suggesting that the presence of this shell is essential for the hydrophobic minimum in the entropy versus charge curves.

The concepts of structure-breaking and structure-making were introduced into the discussion of ion solvation by Frank and Evans[15–17] to explain the observed variation of entropies of solvation of simple ions in solution. Other thermodynamic properties that have been interpreted by invoking these concepts are the shift in the temperature of maximum density of water due to the presence of ions,[51] the ionic contribution to the heat capacities of aqueous solutions[52] and the trends in the activity coefficients of ionic solutions.[53,54] Transport properties such as the fluidity of electrolyte solutions[17] and the heats of transport of ions in solution[55,56] have also been rationalized on the basis of structural changes produced by dissolved electrolytes.

Most singly charged ions are said to be ''structure-breaking'' as they have positive entropies of solvation compared to the H^+ ion. Doubly charged ions and larger ions (such as tetramethyl ammonium[52]) are described as ''structure-making'' with negative entropies of solvation relative to H^+. Our calculations show clearly the change from structure-breaking to structure-making as the magnitude of the charge is increased at constant size, in agreement with the experimentally observed low entropy of doubly charged ions when compared with singly charged ions. Although the entropy of these hydrophilic solutes is lower than that of the hydrophobic solutes, the free energy of solvation of these solutes is dominated by the energy term which decreases rapidly with charge. It is only for hydrophobic solutes that entropy dominates the solvation free energy.

The variation of solvation entropy with size is different for charges of $+1$ and -1. In both cases the entropy initially increases with size and then reaches a maximum and turns over. In this model the entropy maximum for positive ions is broad covering the ions Na^+, K^+, Rb^+, and Cs^+. We attribute this behaviour to a change from the type of structure-making due to hydrophilic ordering for small ions to the incompatible hydrophobic ordering for large ions. Ions with a large local field (those that have a high charge or a small size) order the water structure into well defined and ordered solvation shells. Ions with a very low local field (large ions or ions with a small charge) behave like uncharged solutes with local hydrophobic order which also extends to at least two well defined solvation shells. However, as we saw from the radial distribution functions, the solvation shells are different in the two cases. Hydrophilic ordering makes shells which are close to the ion and which contain a small number of water molecules oriented towards or away from the ion while hydrophobic solvation shells tend to be further from the solute and to contain more molecules. These structures are incompatible and as we vary either the solute size or the solute charge the entropy increases to a maximum at the change over from hydrophilic to hydrophobic order. This change over corresponds to the extreme of structure-breaking. The maximum in entropy as a function of ion size occurs at a larger radius for negative ions than for positive ions, so that common monatomic negative ions have a smaller entropy of solution than do common monoatomic positive ions of the same size.

B. The origin of the asymmetry between positive and negative charged solutes

In a pure dipolar solvent there would be no difference between positive and negative ions of the same size. The local field near a small spherical solvent is far from uniform and in order to understand the molecular orientation one must take into account the higher multipole moments of the charge distribution in the water molecule as well as the influences of hydrogen-bonds between water molecules. In the SPC/E model the internal charge distribution is modelled by charges on the proton and oxygen sites. This model is by no means perfect, but does contain a more realistic picture of the electrostatic potential outside the molecule than would be given by a simple point dipole. An important aspect of the charge distribution is that the proton sites are near the outside of the molecule, so that a negative charge can approach one of the protons closely, while a positively charged ion cannot get as near the negatively charged oxygen site. This means that the interaction of a small negative ion with water molecules in the first solvation shell is much stronger than the interaction of a positively charged ion of the same size. Although this may be overestimated in the SPC/E model and others in which the repulsion is spherical, it is a real effect which is closely related to the ability of the proton of the water to form hydrogen bonds. Because a hydrogen-bond acceptor can approach more closely to a proton in a hydrogen-bond donor than to other types of electropositive atoms in molecules, it interacts particularly strongly with the proton.

C. Comparison with experiment and with other calculations

As has been emphasized earlier the results we have quoted refer only to the local contributions to the entropy and free energy. The usual method for correcting for finite size effects is to add a Born correction, but we follow Hummer *et al.*[27] and the discussion in Section II A. For our system size the finite size corrections are equal $-160q^2$ kJ mol^{-1} to the free energy and -1 k to the entropy for solutes with charge $q=\pm 1$. Note that these corrections are independent of the solute size. Table II shows the values of the raw data for A_{solv} from our simulations, corrected values and experimental numbers.[57,27,44] The agreement with experiment is satisfactory, particularly for the values of the free energy. Although the values of the entropy are in broad agreement with experimental observations, the detailed variation with size are not well reproduced. It seems that the maximum in the variation of ion entropy with size occurs at somewhat too small a value compared to real ions. Either the hydrophobic ordering is overestimated or the hydrophilic ordering is underestimated in this model.

TABLE II. Solvation free energies and entropies as measured in this work and experimental values.

Ion	A_{solv}/kJ mol^{-1} (raw)	(corrected)[a]	(exp)[b]	S_{solv}/k (raw)	(corr)	(exp)[c]
Na^+	−187	−347	−365	−6	−7	−12.0
K^+	−117	−277	−295	−6	−7	−8.1
Cs^+	−74	−234	−235	−7	−8	−6.0
Cl^-	−200	−360	−340	−7	−8	−10.1
I^-	−131	−291	−254	−9	−10	−5.5

[a]See text.
[b]References 57, 38, and 27. These assume a value of −1050 kJ mol^{-1} for H^+.
[c]Reference 58; the absolute values assume a value of −14.55 for H^+ and are less accurate than the relative values.

D. Limitations of the model and of these calculations

The main limitations are in the form of the potential and in the size of the system and the use of periodic boundary conditions to describe an infinite system. All models have their limitations and we are well aware that SPC/E water with charged Lennard-Jones spheres as solutes does not describe all experimental properties in a satisfactory way. This we believe is less important for a study like this where our primary interest is in trends and understanding rather than in detailed comparison of specific systems with experiment. Thus, while the extent of hydrogen-bonded structure around a solute may not be described exactly, we anticipate that trends as a function of solvent size and charge are described correctly. In fact the SPC/E potential has proved reasonably successful in describing many aspects of bulk water, and the water–ion potentials used in this work have been shown to give reasonable values for the mobilities of a range of ions. However the model does not include polarisability which could be important near charged ions — especially for the smaller ions studied here.

The other possible problem with these simulations is the use of periodic boundaries to model an infinite system so that the actual simulation cell is small and the finite size corrections large. The question is whether the particular effects due to the molecular nature of the solvent as opposed to a uniform medium are included. Using fcc periodic boundary conditions gives a truncated dodecahedral simulation cell approximately spherical in shape. In these simulations the minimum diameter is 13.902 18 Å which is smaller than the cell used by Lee and Rasaiah.[7] Lee and Rasaiah found that the radial distribution functions for both ion–oxygen and ion–hydrogen separations had decayed to unity for all the positive ions and was close to unity for the negative ions by $r=7$ Å, so this seemed to be a reasonable choice. However for the largest family of ions studied here (I^-) we find that this may be somewhat too small a value to include the second solvation shell of the neutral species, which may lead to a misestimate of the entropy of solvation for this species.

E. Conclusions

These calculations show that the phenomena associated with hydrophobic and hydrophilic solvation and, in particular, entropic effects can be described using very simple classical model potentials and small system sizes. The essential physics of solvation must be present in these models, although details such as solvent polarisation are omitted. Even in these models, the electrostatic field of a water molecule is more complex than dipolar and is by no means symmetrical under the combined operation of charge conjugation and molecular inversion. This leads to hydrogen-bonding, local solvation structures and to asymmetries in the energetics of positive and negatively charged ions. Structure-breaking is an old concept which has been fleshed out by these calculations; in particular they draw attention to the importance of the second hydration shell.

ACKNOWLEDGMENTS

We thank the University of Maine for a Libra Visiting Professorship (RML-B), EPSRC for financial support (Grants Nos. GR/K20651 and GR/L08427) and the International Fund for Ireland for support for the Irish Centre for Colloids and Biomaterials. J.C.R. is supported by the National Science Foundation under Grant No. CHE-9610288.

[1] F. Franks, *Water, A Comprehensive Treatise* (Plenum, New York, 1973), Vol. 3.
[2] H. Eisenberg and W. Kauzmann, *The Structure and Properties of Water* (Oxford, Oxford, 1969).
[3] G. A. Jeffrey, *An Introduction to Hydrogen Bonding* (Oxford, Oxford, 1997).
[4] C. Tanford, *The Hydrophobic Effect*, 2nd ed. (Wiley, New York, 1980).
[5] A. Ben-Naim, *Hydrophobic Interactions* (Plenum, New York, 1980).
[6] F. H. Stillinger, Adv. Chem. Phys. **321**, 1 (1975); Science **209**, 451 (1980).
[7] S. H. Lee and J. C. Rasaiah, J. Chem. Phys. **100**, 1420 (1996); J. Chem. Phys. **101**, 6964 (1994).
[8] P. G. Wolynes, J. Chem. Phys. **68**, 473 (1978); P. Colonomos and P. G. Wolynes, J. Chem. Phys. **71**, 2644 (1979); J. Hubbard, and P. Wolynes, *The Chemical Physics of Ion Solvation*, Part C. edited by R. R. Dogonadze, E. Kalman, A. A. Kornyshev, and J. Ulstrup (Elsevier, New York, 1985); J. Hubbard, in *The Physics and Chemistry of Aqueous Ionic Solutions*, edited by M. C. Bellisent-Funel and G. W. Neilson (D. Reidel, New York, 1987).
[9] R. Biswas, S. Roy, and B. Bagchi, Phys. Rev. Lett. **75**, 1098 (1995).
[10] A. Yoshimori, Chem. Phys. Lett. **225**, 494 (1994).
[11] R. W. Impey, P. A. Madden, and I. R. McDonald, J. Phys. Chem. **87**, 5071 (1983).
[12] C. Pengali, M. Rao, and B. J. Berne, J. Chem. Phys. **71**, 2795 (1979).
[13] A. D. J. Haymet, Ann. (N.Y.) Acad. Sci. **715**, 146 (1993).
[14] A. D. J. Haymet, K. A. Silverstein, and K. A. Dill, Faraday Discuss. **103**, 117 (1996).
[15] H. S. Frank, J. Chem. Phys. **72**, 2384 (1980).
[16] H. S. Frank and M. W. Evans, J. Chem. Phys. **13**, 507 (1945).
[17] R. W. Gurney, *Ionic Processes in Solution* (McGraw-Hill, New York, 1953; Dover, New York, 1962).
[18] D. Frenkel and B. Smit, *Understanding Molecular Simulation* (Academic, San Diego, 1996).
[19] T. P. Straatsma and J. A. McCammon, Annu. Rev. Phys. Chem. **43**, 407 (1992).
[20] G. M. Torrie and J. P. Valleau, J. Comp. Physiol. **23**, 187 (1977).
[21] See articles by P. M. King, W. F. van Gunsteren *et al.*, and T. P. Straasma, W. F. Zacharias and J. A. McCammon, in *Computer Simulation of Biomolecular Systems*, edited by W. F.van Gunsteren, P. K. Weiner, and A. J. Wilkinson (ESCOM, Leiden, 1993), Vol. 2.
[22] C. Reynolds, P. M. King, and W. G. Richards, Mol. Phys. **76**, 251 (1992).
[23] B. Tembe and J. McCammon, Comput. Chem. **8**, 281 (1984).
[24] J. P. M. Potsma, H. J. C. Berendsen, and J. R. Haak, Faraday Symp. **17**, 55 (1981).

[25] T. P. Lybrand, I. Gosh, and J. A. McCammon, J. Am. Chem. Soc. **107**, 7793 (1985).
[26] W. L. Jorgensen, J. F. Blake, and J. K. Buckner, Chem. Phys. **129**, 193 (1989).
[27] G. Hummer, L. R. Pratt, and A. E. García, J. Phys. Chem. **100**, 1206 (1996).
[28] S. G. Kalko, G. Sesé, and J. A. Padró, J. Chem. Phys. **104**, 9578 (1996).
[29] W. L. Jorgensen and C. Ravimohan, J. Chem. Phys. **83**, 3050 (1985).
[30] T. P. Straatsma, H. J. C. Berendsen, and J. P. M. Potsama, J. Chem. Phys. **85**, 6720 (1986).
[31] B. Guillot, Y. Guissani, and S. Bratos, J. Chem. Phys. **95**, 3643 (1991).
[32] D. E. Smith and A. D. J. Haymet, J. Chem. Phys. **98**, 6445 1993.
[33] A. Wallquist and B. J. Berne, J. Phys. Chem. **99**, 2885 (1995).
[34] P.-L. Chau, T. R. Forester, and W. Smith, Mol. Phys. **89**, 1033 (1996).
[35] C. H. Bridgeman, A. D. Buckinham, and N. T. Skipper, Chem. Phys. Lett. **253**, 209 (1996).
[36] P. A. Bash, U. C. Singh, R. Lamgridge, and P. A. Kollman, Science **236**, 564 (1987); U. C. Singh, F. K. Brown, P. A. Bash, and P. Kollmann, J. Am. Chem. Soc. **109**, 1607 (1987).
[37] R. A. Robinson and R. H. Stokes, *Electrolyte Solutions*, 2nd ed. (Butterworth, London, 1959).
[38] P. W. Atkins, *Physical Chemistry*, 5th ed. (W. H. Freeman, New York, 1994).
[39] J. Israelachvilli, *Intermolecular and Surface Forces* (Academic, New York 1992).
[40] G. A. Vidulich and R. L. Kay, J. Phys. Chem. **60**, 383 (1962).
[41] B. Cichocki, B. U. Felderhof, and K. Hinsen, Phys. Rev. A **39**, 5350 (1989).
[42] This was calculated using data in Ref. 41.
[43] H. C. Anderson, J. Chem. Phys. **72**, 2384 (1980).
[44] M. P. Allen and D. J. Tildesley, *Computer Simulation of Liquids* (Oxford, Oxford, 1987).
[45] S. Nosé, Mol. Phys. **52**, 187 (1986).
[46] R. Car and M. Parrinello, Phys. Rev. Lett. **55**, 2471 (1985).
[47] H. J. C. Berendsen, J. R. Grigera, and T. P. Straatsma, J. Phys. Chem. **91**, 6269 (1987).
[48] L. X. Dang, Chem. Phys. Lett. **200**, 21 (1992); L. X. Dang and B. C. Garrett, J. Chem. Phys. **99**, 2972 (1993); D. E. Smith and L. X. Dang, *ibid.* **100**, 3757 (1994); L. X. Dang, Chem. Phys. Lett. **227**, 211 (1994); L. X. Dang and P. A. Kollman, J. Phys. Chem. **99**, 55 (1995); L. X. Dang, J. Am. Chem. Soc. **117**, 6954 (1995); L. X. Dang, J. Chem. Phys. **96**, 6970 (1992).
[49] R. M. Lynden-Bell and J. C. Rasaiah, J. Chem. Phys. **105**, 9266 (1996).
[50] T. R. Forester and W. Smith, DL_POLY_2.4, Daresbury Laboratory U.K., 1995.
[51] H. S. Frank and A. L. Robinson, J. Chem. Phys. **8**, 933 (1940).
[52] H. S. Frank and W. Wen, Discuss. Faraday Soc. **24**, 133 (1957).
[53] J. C. Rasaiah, J. Chem. Phys. **52**, 704 (1970); J. C. Rasaiah, J. Soln. Chem. **2**, 301 (1973).
[54] P. S. Ramanathan and H. L. Friedman, J. Chem. Phys. **54**, 1086 (1971).
[55] J. N. Agar and J. C. R. Turner, Proc. Phys. Soc. London, Sec. A Electrolyte solutions, edited by W. J. Hamer (Wiley, New York, 1959), Chap. 13.
[56] H. S. Frank, *Chemical Physics of Ionic Solutions*, edited by B. E. Conway and R. G. Barradas (Wiley, New York, 1956), Chap. 4.
[57] Y. J. Marcus, J. Chem. Soc. Faraday Trans. **87**, 2997 (1991).
[58] A. G. Sharpe, *Inorganic Chemistry*, 2nd ed. (Longman, London, 1986).